Finite-temperature vortex dynamics in Bose-Einstein condensates

B. Jackson,[1,*] N. P. Proukakis,[1] C. F. Barenghi,[1] and E. Zaremba[2]
[1]*School of Mathematics and Statistics, Newcastle University, Newcastle upon Tyne NE1 7RU, United Kingdom*
[2]*Department of Physics, Engineering Physics and Astronomy, Queen's University, Kingston, Ontario, Canada K7L 3N6*
(Received 10 July 2008; revised manuscript received 15 April 2009; published 12 May 2009)

We study the dynamics of a vortex in an atomic Bose-condensed gas at finite temperature within the Zaremba-Nikuni-Griffin formalism. In a harmonically trapped pancake-shaped condensate, an off-centered vortex is known to decay by spiraling out toward the edge of the condensate. We quantify the dependence of this decay on temperature, atomic collisions, and thermal cloud rotation. Near the trap center where the density varies slowly, we show that our numerical results agree with the predictions of the Hall-Vinen phenomenological friction force model used to describe quantized vorticity in superfluid systems. Our result thus clarifies the microscopic origin of the friction and provides an *ab initio* determination of its value.

DOI: 10.1103/PhysRevA.79.053615 PACS number(s): 03.75.Kk, 03.75.Lm, 67.25.dk

I. INTRODUCTION

The dynamics of Bose-Einstein condensates (BEC) at finite temperature presents an interesting problem in the study of ultracold Bose gases. In most experiments, such systems are only partially condensed, with the noncondensed thermal cloud providing a source of dissipation and leading to damping of excitations such as collective modes [1–4], solitons [5], and vortices [6,7]. Several approaches have been developed to describe these systems, including phenomenological models [8,9], generalized mean-field treatments [10–15], number-conserving approaches [16–18], classical field theory [19–21], and stochastic approaches [22–24], as recently reviewed by two of the authors [25], who give a more complete list of references (see also [26]). Although the underlying theory is well understood, the implementation of models which can be actually solved in specific contexts has proven to be a considerable challenge, with the majority of treatments to date assuming the thermal cloud to be homogeneous and static.

In this paper we use the formalism of Zaremba, Nikuni, and Griffin (ZNG) [12]. The ZNG theory is a kinetic approach in which a generalized Gross-Pitaevskii (GP) equation for the condensate order parameter is coupled to a Boltzmann equation for the thermal cloud. These equations have already been solved numerically [27] and applied to the study of collective modes [28–30], the hydrodynamic regime [31,32], and the decay of dark solitons [33], demonstrating good agreement with experiments.

At zero temperature, the collective excitations of a harmonically trapped condensate with a central vortex can be determined by solving the Bogoliubov equations [34]. One particular excitation, the so-called "anomalous" mode, was subsequently explained to represent the precession of an off-centered vortex [35]. This mode can also be obtained using a Lagrangian formalism [35,36] which makes it clear that the vortex moves with a constant energy on a circular trajectory of constant radius. At finite temperature the presence of dissipation leads to the vortex minimizing its energy by moving toward the surface, where it eventually leaves the condensate and disappears. This decay has been observed experimentally [6,7], but the precise theoretical modeling of this process has proven rather challenging. The primary aim of this paper is to apply the ZNG model to this problem.

Our approach should be contrasted with earlier work. Dissipation based on the scattering of single-particle excitations from the mean-field potential at the vortex core was considered by Fedichev and Shlyapnikov [37] and was subsequently extended to treat vortex lattices [38,39]. The problem of vortex nucleation was then considered by Penckwitt *et al.* [40] using an approximation in which the thermal cloud is treated as *static*. Schmidt *et al.* [41] were the first to apply the classical field method to the problem of vortex decay, while more recent applications of the method addressed vortex dynamics in quasi-two-dimensional systems [42,43]. Duine *et al.* [44] considered the dynamics of a straight vortex line using a closely related method based on a stochastic Gross-Pitaevskii equation [23] and derived a stochastic equation of motion for the position of the vortex core; a similar equation was also used by Šášik *et al.* [45] to numerically simulate the motion of an isolated vortex in a uniform box with periodic boundary conditions. Compared to the literature cited above, our work represents the microscopic simulations which fully account for the dynamics of an inhomogeneous thermal cloud.

Our work, however, also has a second motivation. Although the topic of quantized vorticity in superfluids is interesting *per se* (as shown by the number of recent vortex experiments in atomic Bose-Einstein condensates), it also has implications in the subject of quantum turbulence [46]. Current work on turbulent superfluid ^{4}He and ^{3}He-*B*, for example, is concerned with the extent to which turbulence in these systems differs from that found in ordinary classical fluids [47–55]. What makes quantum fluids attractive from the point of view of understanding the principles of turbulence is the existence of various forms of dissipation which are distinct from ordinary viscosity. At sufficiently low temperatures, kinetic energy can be dissipated into sound waves, which is phonons [56], via a Kelvin wave cascade [57] or via vortex reconnections [58]. At higher temperatures, the friction force [59] between the superfluid and the normal fluid

*Deceased.

component can change the nature of the turbulent kinetic energy cascade. For example, in the classical turbulence scenario [60], the Richardson-Kolmogorov inertial cascade is limited at large wave numbers where viscous dissipation destroys the small scales, whereas in superfluid ^{3}He-B at relatively high temperatures the friction can limit the inertial cascade at small wave numbers [61].

The mutual friction between a superfluid and a normal fluid is one of the most intricate issues of superfluidity [62]; in particular, the existence of a transverse force on quantized vortices parametrized by a dimensionless temperature dependent quantity called α' has been controversial [63–66]. Studying vortex motion in an atomic BEC at finite temperatures, and interpreting the results from the point of view of vortex dynamics, allows one to compute the friction force directly from first principles. However, in order to do this in a meaningful way for a harmonically trapped, which is inhomogeneous BEC, we must restrict our analysis to vortices close to the center of the trap where the density is nearly constant. Undertaking such an analysis provides insights into the important problem of mutual friction which cannot be obtained as readily with superfluid helium.

This paper is structured as follows. Section II briefly reviews the ZNG theoretical model and numerical implementation. Section III presents our main findings on vortex decay (Sec. III A) and highlights the dependence of the friction coefficients on system parameters for vortices located initially near the trap center (Sec. III B). The role of collisions between the atoms (Sec. III C) and the effect of thermal cloud rotation (Sec. III D) are also considered. Section IV presents some concluding remarks and briefly discusses the implications of our analysis for the motion of vortex lattices.

II. THEORY

A. ZNG formalism

Following Refs. [12,27], the second-quantized field operator $\hat{\psi}(\boldsymbol{r},t)$ can be split into condensate and thermal contributions. Making use of Bose broken symmetry, the full operator is written as $\hat{\psi}(\boldsymbol{r},t)=\Psi(\boldsymbol{r},t)+\tilde{\psi}(\boldsymbol{r},t)$, where $\Psi(\boldsymbol{r},t)=\langle\hat{\psi}(\boldsymbol{r},t)\rangle$ is the condensate wave function (angular brackets denote an expectation value) and $\tilde{\psi}(\boldsymbol{r},t)$ is the noncondensate field operator. Starting with the Heisenberg equation of motion for $\hat{\psi}(\boldsymbol{r},t)$, one eventually arrives at the following pair of equations:

$$i\hbar\frac{\partial\Psi}{\partial t}=\left(-\frac{\hbar^2\nabla^2}{2m}+V+gn_c+2g\tilde{n}-iR\right)\Psi, \tag{1}$$

$$\frac{\partial f}{\partial t}+\frac{\boldsymbol{p}}{m}\cdot\nabla f-\nabla U\cdot\nabla_{\boldsymbol{p}}f=C_{12}+C_{22}. \tag{2}$$

Equation (1) is a generalized GP equation for the condensate wave function $\Psi(\boldsymbol{r},t)$ and has been obtained in the so-called "Hartree-Fock-Popov" approximation [10], whereby the static value of the anomalous average, which is responsible for certain many-body effects [67–70], is ignored. Equation (2) is a Boltzmann equation for the thermal cloud phase space density $f(\boldsymbol{p},\boldsymbol{r},t)$, with thermal energies calculated in the Hartree-Fock approximation [71]. The condensate density is defined as $n_c=|\Psi|^2$, while the thermal cloud density is obtained from f by means of the momentum integral $\tilde{n}=\int(d\boldsymbol{p}/h^3)f$. The mean-field interactions between atoms is parametrized by $g=4\pi\hbar^2a/m$, where m is the atomic mass and a is the s-wave scattering length. The thermal atoms experience an effective potential given by $U(\boldsymbol{r})=V(\boldsymbol{r})+2g(n_c+\tilde{n})$, where $V(\boldsymbol{r})=m(\omega_\perp^2r^2+\omega_z^2z^2)/2$ represents the external trap.

The terms involving gn_c and $g\tilde{n}$ in Eq. (1) and ∇U in Eq. (2) represent mean-field couplings between atoms in the condensate and the thermal cloud. This coupling is a source of dissipation for the system and gives rise, for example, to Landau damping of collective modes [72–75]. The ZNG model also includes "collisional integrals" C_{22} and C_{12}, which denote binary collisions between noncondensate atoms and between condensate and noncondensate atoms, respectively. They are given by

$$\begin{aligned}C_{22}=\frac{2g^2}{(2\pi)^5h^7}\int d\boldsymbol{p}_2d\boldsymbol{p}_3d\boldsymbol{p}_4\\ \times\delta(\boldsymbol{p}+\boldsymbol{p}_2-\boldsymbol{p}_3-\boldsymbol{p}_4)\delta(\epsilon+\epsilon_2-\epsilon_3-\epsilon_4)\\ \times[(1+f)(1+f_2)f_3f_4-ff_2(1+f_3)(1+f_4)],\end{aligned} \tag{3}$$

$$\begin{aligned}C_{12}=\frac{2g^2n_c}{(2\pi)^2h^4}\int d\boldsymbol{p}_2d\boldsymbol{p}_3d\boldsymbol{p}_4\\ \times\delta(m\boldsymbol{v}_c+\boldsymbol{p}_2-\boldsymbol{p}_3-\boldsymbol{p}_4)\delta(\epsilon_c+\epsilon_2-\epsilon_3-\epsilon_4)\\ \times[\delta(\boldsymbol{p}-\boldsymbol{p}_2)-\delta(\boldsymbol{p}-\boldsymbol{p}_3)-\delta(\boldsymbol{p}-\boldsymbol{p}_4)]\\ \times[(1+f_2)f_3f_4-f_2(1+f_3)(1+f_4)],\end{aligned} \tag{4}$$

where $f\equiv f(\boldsymbol{p},\boldsymbol{r},t)$ and $f_i\equiv f(\boldsymbol{p}_i,\boldsymbol{r},t)$. In the above expressions, delta functions enforce momentum and energy conservation in the collisions, where $\epsilon=p^2/(2m)+U$ is the thermal atom energy (in the Hartree-Fock limit), $\epsilon_c=mv_c^2/2+\mu_c$ is the local condensate energy, with $\boldsymbol{v}_c=\hbar(\Psi^*\nabla\Psi-\Psi\nabla\Psi^*)/(2imn_c)$, and μ_c is the chemical potential.

The C_{12} term [Eq. (4)] involves those collisions between condensate and thermal atoms which lead to a transfer of atoms between condensate and thermal cloud. This term is thus related to the source term $-iR\Psi$ appearing in Eq. (1) via

$$R(\boldsymbol{r},t)=\frac{\hbar}{2n_c}\int\frac{d\boldsymbol{p}}{(2\pi\hbar)^3}C_{12}. \tag{5}$$

If R is positive (negative), there is a net local flux of atoms *out of* (*into*) the condensate.

B. Numerical methods

The methods used for our numerical simulations are discussed more fully in Ref. [27] and are only briefly reviewed here.

First, we must generate a suitable initial state for the simulations which consists of a condensate in equilibrium with a thermal cloud at temperature T. The condensate wave function can be obtained by an imaginary time propagation

$(t \rightarrow -it)$ of Eq. (1) with $R=0$. The thermal cloud density $\tilde{n}=0$ is first set to zero, and an approximate thermal cloud potential $U \simeq V+2gn_c$ is constructed from the self-consistently determined condensate wave function. This yields the initial thermal cloud density $\tilde{n}_0(\boldsymbol{r})=(1/\Lambda^3)g_{3/2}(z)$, where $\Lambda=(2\pi\hbar^2/mk_BT)^{1/2}$ is the thermal de Broglie wavelength, $z(\boldsymbol{r})=\exp\{\beta[\mu_c-U(\boldsymbol{r})]\}$ is the local fugacity, and μ_c is the condensate chemical potential. This density is then used in Eq. (1) to obtain an improved condensate wave function and the procedure is iterated until a self-consistent solution of both the condensate and thermal cloud densities is obtained. (For more details see [27].)

The vortex state of interest in our simulations can be obtained from this equilibrium state by multiplying the condensate wave function by the phase factor $\exp[iS(\boldsymbol{r})]$, where $S(\boldsymbol{r})=\arctan[(y-y_0)/(x-x_0)]$, which imprints the velocity field of a straight vortex located at (x_0,y_0). The GP equation is then evolved again in imaginary time for a short period until a fully developed vortex in the condensate is formed and most short-time-scale transients in the initial configuration (for example, phonon excitations) have damped out.

The state generated in this way is a quasiequilibrium state containing one vortex whose subsequent dynamical evolution is of interest. The generalized Gross-Pitaevskii equation for the condensate wave function (1) can be solved readily in real time using standard methods [76], in our case a split-operator fast Fourier transform approach on a three-dimensional (3D) Cartesian grid. The thermal cloud is described by a swarm of classical test particles which move in an external potential $U(\boldsymbol{r},t)$ and which can collide with each other or with the condensate in each time step. The probabilities of particle collisions are chosen so that they correspond to a Monte Carlo evaluation of the collision integrals in Eqs. (3) and (4). Together with the Newtonian dynamics of the test particles, this procedure is equivalent to solving the collisional Boltzmann equation [Eq. (2)]. The C_{12} probabilities are then summed according to Eq. (5) to determine $R(\boldsymbol{r},t)$, which appears in the GP equation [Eq. (1)]. Since $R(\boldsymbol{r},t)$ is a non-Hermitian term, it leads to a change in the normalization of the wave function, corresponding to condensate growth or loss, which is accompanied by a compensating removal or creation of thermal particles. An essential ingredient in the simulations is the evaluation of the thermal cloud density $\tilde{n}(\boldsymbol{r},t)$, which appears in both Eqs. (1) and (2) (through the effective potential U). This is achieved by appropriately binning the thermal particles and then convolving the binned distribution with a Gaussian in order to obtain a smoothly varying density.

III. RESULTS

We start our analysis by investigating the dynamics of a single vortex in a pancake-shaped condensate with $N=10^4$ ^{87}Rb atoms with trap frequencies $\omega_\perp=2\pi\times 129$ Hz and $\omega_z=\sqrt{8}\omega_\perp$. This geometry has the advantage that the extent of the condensate in the axial direction is much smaller than in the radial, so that the vortex remains relatively straight throughout its motion. This simplifies the analysis considerably, as the vortex dynamics can be characterized by just its x and y coordinates. For the chosen parameters, the (ideal gas) critical temperature is $T_c=177$ nK.

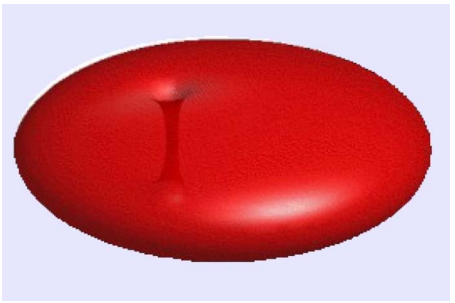

FIG. 1. (Color online) Three-dimensional density isosurface showing an off-centered vortex in a pancake-shaped condensate.

A. Vortex decay

We consider an off-centered vortex which is initially located relatively close to the center; for example, following the initial preparation phase, the vortex is centered at $x_v(0)\simeq 1.3a_\perp$, $y_v(0)=0$, as illustrated in Fig. 1, where $a_\perp=\sqrt{\hbar/m\omega_\perp}$ is the harmonic oscillator length in the radial direction. The subsequent vortex position $\mathbf{r}_v(t)=(x_v(t),y_v(t))$ is tracked by finding the local minimum of the vortex core density in the $z=0$ plane by means of a quadratic interpolation between grid points. This procedure breaks down when the vortex enters the very low density region at the edge of the condensate [typically at distances $\geq 3x_v$ (0) for the temperature range considered below], so no results are shown when this happens. This condition can be taken as the point at which the vortex "disappears" from the condensate and would correspond in the experimental context to the density contrast of the vortex being below the detection limit. Since the initialization process induces a center-of-mass motion of the condensate, throughout this paper we only discuss the vortex position relative to the center-of-mass position, as this represents the most interesting vortex dynamics.

Simulations of the GP equation for $T=0$ reveal that the vortex precesses in a circular path around the condensate, following a trajectory of constant energy as would be expected for a nondissipative system. This well-known precessional behavior can be understood as arising from the nonuniform density of the condensate, which means that the energy of the vortex is a function of its radial position. Hence there is an effective Magnus force, proportional to the gradient of the energy and directed radially, which in turn induces the azimuthal vortex motion [77]. This can be described quantitatively by means of a time-dependent variational method [35,36,78]. In addition to the motion described above, the acceleration experienced by the vortex in its circular trajectory can, in principle, lead to the emission of sound waves. However, for the harmonic confinement being considered, any emission of sound waves is followed by reabsorption, and no net dissipation occurs. There is nevertheless some modulation of the vortex trajectory arising from the dynamical interaction between the vortex and sound waves [79].

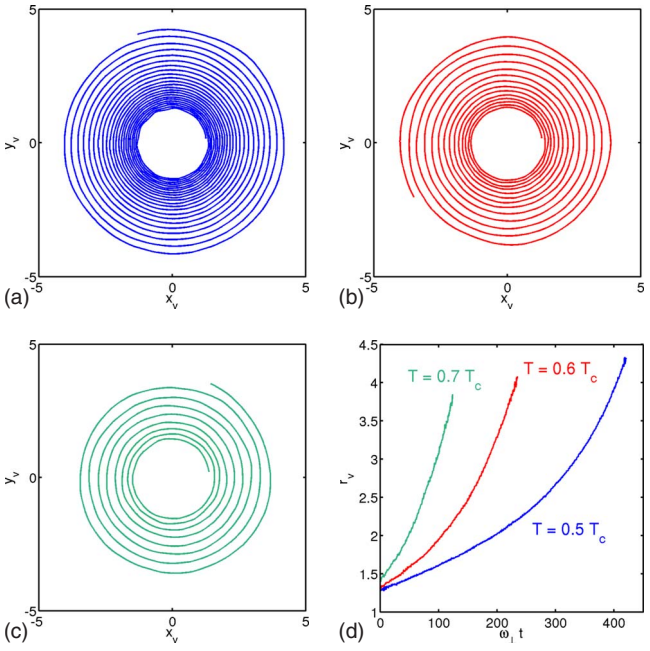

FIG. 2. (Color online) Position of the vortex (x_v, y_v) (in units of $a_\perp = \sqrt{\hbar/m\omega_\perp}$) as it spirals out of the condensate at $T=0.5T_c$ (top left, blue), $T=0.6T_c$ (top right, red), and $T=0.7T_c$ (bottom left, green) for a vortex initially located at $(1.3a_\perp, 0)$. At the bottom right, the radial position r_v of the vortex is plotted versus $\omega_\perp t$ for each temperature. The trap parameters are $\omega_\perp = 2\pi \times 129$ Hz and $\omega_z/\omega_\perp = \sqrt{8}$, with $N = 10^4$ ^{87}Rb atoms.

In contrast to this dissipationless motion at $T=0$, the vortex can lose energy at finite temperatures due its interaction with the thermal component, and as a result, it moves outward radially toward the condensate edge. The resulting spiral trajectory is illustrated in Fig. 2 for temperatures $T=0.5T_c$, $T=0.6T_c$, and $T=0.7T_c$. The bottom-right part of Fig. 2 shows the outward relaxation of the radial position $r_v = |\mathbf{r}_v| = \sqrt{x_v^2 + y_v^2}$ as a function of time for the three temperatures. The figure demonstrates, as one would expect, that the relaxation rate increases with temperature; in order to minimize the effects of the inhomogeneous density, we analyze in the following the short-time behavior of these curves.

As well as monitoring the vortex position, it is instructive to examine the evolution of the density distributions themselves during the simulation. The top panel in Fig. 3 shows the condensate density cross section at $z=0$ for various times and for a temperature of $T=0.7T_c$. The vortex core (dark) in the condensate images is observed to precess in a circle; approximately one period of this precessional motion is shown. The bottom panel in Fig. 3 shows the thermal cloud density. As this is much smaller than the condensate density, a different color scale is used here for clarity but with red still indicating high densities. The ring of high density at the edge of the condensate is due to the fact the effective potential $U(\boldsymbol{r}, t)$ has a minimum in this region. In addition, the thermal cloud density has a peak at the position of the vortex core. The low condensate density in the core of the vortex reduces the mean-field repulsion experienced by the thermal atoms and as a result, the thermal atoms tend to "fill in" the vortex core. It is interesting to note that this peak in the

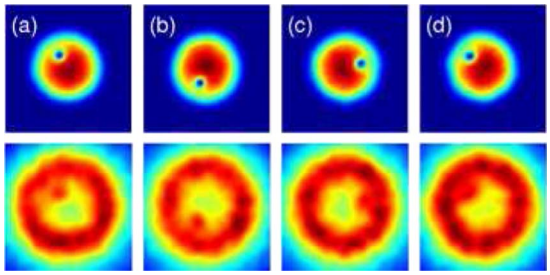

FIG. 3. (Color online) Density cross sections of the condensate (top row) and thermal cloud (bottom row) at $z=0$ for $T=0.7T_c$ and at the times (a) $\omega_\perp t=6$, (b) 12, (c) 18, and (d) 24. The colors range from brown or red (high density) to dark blue (low density), with different scales for the condensate and thermal cloud densities.

thermal cloud density tends to follow the core as it precesses and spirals out. Furthermore, the sense of precession is the *same* as for the pure condensate in the $T=0$ limit. This behavior is in contrast to what is found [80] when the dynamics of the thermal cloud is not taken into account self-consistently as in the present work. In the Hartree-Fock-Popov-Bogoliubov approximation [80], the static thermal cloud density effectively provides a pinning potential [81], and as a result, the lowest $m=-1$ excitation frequency has a sign opposite to that found at $T=0$. This leads to the opposite sense of precession of the vortex core. It is thus clear that the fully self-consistent dynamics of the thermal cloud is essential if the observed sense of precession [82] is to be reproduced.

Close to the trap center, we find that the radial position of a vortex exhibits a near-exponential growth in time. This is evident from the inset of Fig. 4, which plots the time evolution of r_v on a logarithmic-linear scale for $T=0.5T_c$ (rather than on a linear-linear scale as in Fig. 2). The inset shows that r_v departs from the exponential behavior only at later times when the vortex approaches the edge of the condensate; similar behavior is found for the other temperatures. To quantify the relaxation near the trap center we thus fit $r_v(t)$ to the function $r_v(t) = r_0 \exp(\gamma t)$ in the time interval $0 \le t \le 50$

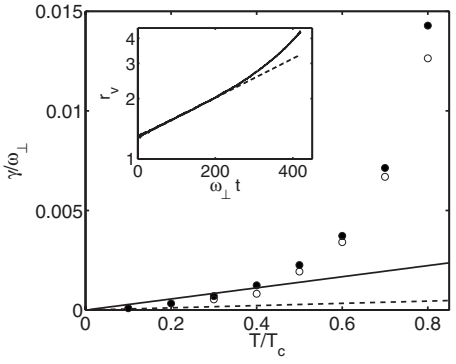

FIG. 4. (Inset) Ln-log plot of the vortex radial position as a function of time for $T=0.5T_c$ (solid line). The dashed line is an exponential fit, $r_v(t) = r_0 e^{\gamma t}$, to the data over $0 \le \omega_\perp t \le 50$. The main figure plots the resulting values of γ for an initial vortex position of $r_0 \simeq 1.3$ (solid circles) and $r_0 \simeq 0.65$ (open circles). For comparison, the solid and dashed lines plot the results of FS [37] and DLS [44], respectively.

when the exponential behavior remains valid for all temperatures under consideration. The resulting values of γ are plotted in the main panel of Fig. 4 with the black circles.

It is important to note that, although deviations from an exponential behavior appear at longer times, the decay rates extracted from the simulations depend only weakly on the initial position of the vortex. In Fig. 4 we show the effect of halving the initial radial vortex displacement from the origin from $r_0=1.3a_\perp$ to $0.65a_\perp$. We observe that the decay rates are slightly smaller when the vortex starts from a position closer to the center of the condensate. This can easily be explained in terms of the smaller thermal cloud density closer to the trap center where the condensate density is a maximum. (Recall that the condensate gives rise to a repulsive mean-field potential acting on the thermal cloud.) Since the vortex is initially moving through a lower thermal cloud density in the $r_0=0.65a_\perp$ case, one would expect the decay rate to be slightly smaller. This effect is of course weak near the trap center where the condensate density is approximately constant. However, a position-dependent relaxation rate γ is in general to be expected and, in fact, becomes particularly evident at later times (inset of Fig. 4) when the vortex nears the edge of the condensate where the thermal cloud density has a maximum (see Fig. 3).

It is of interest to compare our results to existing analytical predictions obtained by Fedichev and Shlyapnikov (FS) [37], and Duine, Leurs, and Stoof (DLS) [44]. Both FS and DLS actually quote the time scale τ for the decay of a vortex from position $r_{\min}$ to $r_{\max}$, but this can be converted to a decay rate using $\tau=\gamma^{-1}\ln(r_{\max}/r_{\min})$. In both of these works the decay of the vortex is found to be exponential, with a rate $\gamma\propto T$ but with different proportionality coefficients due to the different approximations made in the two theories (see below for the role of the noise term in the DLS analysis). These rates are displayed in Fig. 4 by solid (FS) and dashed (DLS) lines. It is apparent that the rates found by FS are comparable to ours at the lower temperatures but differ significantly at higher T due to the stronger (approximately quadratic) temperature dependence found in our simulations.

FS assumed a uniform condensate in a cylindrical container and modeled the decay solely as the result of mean-field interactions. The DLS study, on the other hand, includes the important C_{12} collisional coupling between the condensate and thermal cloud. With the aim of obtaining analytical results, they approximate the condensate density profile by a Gaussian which is reasonably accurate for the most relevant region near the center of the trap [83]. In this regard, it should be noted that such an approximation has been shown to produce correct results for the frequencies of collective modes even for Thomas-Fermi condensates [84]. Our present simulations, which include both mean-field and collisional coupling mechanisms, enable us to assess their relative importance, which will be discussed in Sec. III C. More importantly, our simulations differ from the other approaches mentioned in that they are actually performed for a dynamical thermal cloud, with both the condensate and thermal cloud densities determined self-consistently during the simulations.

For completeness, we should however make two additional remarks regarding the DLS approach. First, in their preceding work, Duine and Stoof [84] argued that enhanced damping of collective modes at higher temperatures could be related to the position dependence of the self-energy (and hence of the damping term $-iR\Psi$), which was ignored in their analytical treatment based on a volume average over the size of the condensate. In the present context, this could partly account [85] for a deviation of the computed damping rate $\gamma/\omega_\perp$ at higher temperatures from the linear behavior seen in Fig. 4. Although such simulations have not been performed to date, the resulting corrections are likely to be smaller than the observed disagreement, whose origin we believe lies primarily in the dynamics of the thermal cloud.

On the other hand, the DLS analysis is actually more general than ours in that it contains an additional noise term in the equation of motion of the vortex. This provides stochastic "kicks" to the vortex and the ensuing Brownian motion allows for the migration of a vortex away from the center of the trap. Were it is not for the noise, a centered vortex would have an infinite lifetime. This would be the case in an exact application of the ZNG theory. However, its numerical implementation in terms of discrete test particles does introduce statistical fluctuations in the thermal cloud density which plays the role of noise. Thus we indeed find in simulations of a centered vortex a finite, albeit long, lifetime [$\omega_\perp\tau\simeq 1000$ for the relatively high temperature of $T=0.7T_c$ as compared to $\omega_\perp\tau\simeq 120$ for $r_v(0)\simeq 1.3a_\perp$]. This long lifetime, however, should not be taken seriously since it depends on the actual number of test particles used in the simulations. The simulation nevertheless makes clear that this "numerical noise" is of secondary importance at larger radii where the direct coupling to the thermal cloud is the dominant dissipative effect. Although it is something to be checked, it is unlikely that the stochastic term makes a significant contribution to the spiraling out of a vortex when it is located far from the trap center.

Finally, it is worth remarking that our computed decay rates (from approximately 0.5 to 3 s^{-1} in the range $T/T_c=0.4-0.6$) are in order-of-magnitude agreement with the decay rates observed for a vortex lattice [7] (approximately $0.3-3$ s^{-1} over the same relative range).

B. Friction coefficients

In order to further understand the origin of this exponential decay, it is instructive to consider the two-fluid hydrodynamics model used to describe superfluid liquid helium [86]. In this context, dissipation arises from the interaction between the quantized vortices and the thermal excitations (phonons and rotons) which form the normal fluid [59,87]. Since the radius of the superfluid vortex core is much smaller than the typical separation between vortices or any other length scale of interest in the flow, the vortex is described in parametric form as a three-dimensional space curve $\mathbf{s}\equiv\mathbf{s}(\xi,t)$, where ξ is the arc length. The resulting equation of motion [88] is

$$\frac{d\mathbf{s}}{dt}=\mathbf{v}_s+\mathbf{v}_i+\alpha\mathbf{s}'\times(\mathbf{v}_n-\mathbf{v}_s-\mathbf{v}_i)-\alpha'\mathbf{s}'\times[\mathbf{s}'\times(\mathbf{v}_n-\mathbf{v}_s-\mathbf{v}_i)], \quad (6)$$

where $\mathbf{s}'=d\mathbf{s}/d\xi$ is the unit tangent along the vortex at the position $\mathbf{s}$, $\mathbf{v}_s$ is any imposed superfluid velocity, $\mathbf{v}_n$ is the normal fluid velocity, and $\mathbf{v}_i$ is the self-induced velocity of the vortex arising from its own curvature, the presence of other vortices, and any inhomogeneity of the fluid. The first two terms on the right-hand side of Eq. (6) state that at $T=0$ the vortex is advected by the local superflow $\mathbf{v}_s+\mathbf{v}_i$. The remaining two terms reflect the fact that, at nonzero T, the normal fluid streaming past the vortex core exerts a force per unit length whose intensity is controlled by the temperature-dependent friction coefficients α and α' [59,89,90].

In turbulent helium, the friction coefficients α and α' play a key role because they account for the mutual friction between the superfluid and the normal fluid and control the transfer of energy between the two fluids at various length scales and hence the nature of the inertial range cascade [48,91]. The first coefficient, α, describes dissipative effects and leads, for example, to the shrinking [59] of a vortex ring or the damping of a Kelvin wave [92]. In the case of rotating helium, α determines the attenuation of second sound waves, so it allows the experimentalist to determine the density of vortex lines [93]. The second coefficient, α', is not dissipative and, in rotating helium, splits a second sound resonance (besides the classical rotational splitting) in a suitably designed cavity [94]. It has been argued [95,96] that the ratio of inertial and dissipative forces, which is called the Reynolds number in the case of ordinary turbulence [60], is simply $\alpha/(1-\alpha')$ in the case of quantum turbulence.

In our case of a pancake-shaped condensate the vortex line remains approximately straight and we can therefore replace $\mathbf{s}$ by the vortex position $\mathbf{r}_v$, while $\mathbf{s}'=\hat{\mathbf{z}}$. Both the condensate and thermal cloud are stationary, and so $\mathbf{v}_s=\mathbf{v}_n=0$. This just leaves $\mathbf{v}_i$, which in this case corresponds to the azimuthal vortex motion induced by the inhomogeneity of the condensate at $T=0$ (hence, $\mathbf{v}_i=v_i\hat{\phi}$). Rewriting Eq. (6) in cylindrical polar coordinates gives for the azimuthal component

$$\omega_v = (1-\alpha')\frac{v_i}{r_v}, \tag{7}$$

where $\omega_v=\dot{\phi}_v$ is the vortex precession frequency at finite T and the dot denotes a time derivative.

To a first approximation we ignore the mutual friction coefficient α'. We then find $\omega_v=v_i/r_v$ and thus obtain for the radial component

$$\frac{dr_v}{dt} = \alpha\omega_v r_v. \tag{8}$$

If α and ω_v are constant, then one simply recovers the exponential behavior discussed in Sec. III A, with $\gamma=\alpha\omega_v$.

In actual fact, α and ω_v would not be expected to be constant during the course of the vortex decay. The condensate and thermal cloud are both nonuniform (implying a dependence of α on position), while ω_v is only constant near the center and increases as the vortex approaches the edge [77]. This latter effect is illustrated in Fig. 5.

However, as shown in the inset of Fig. 4, Eq. (8) is a good approximation for a significant part of the evolution: the exponential fit is a reasonable approximation up to a value of r_v that is twice the initial value. Thus, by restricting our analysis to vortices with small offsets from the trap center ($r_0 \ll R_\perp$, where $R_\perp$ is the spatial extent of the condensate in the radial direction for a particular temperature), the value of the friction that we deduce is largely independent of the nonuniformity of the density of the condensate.

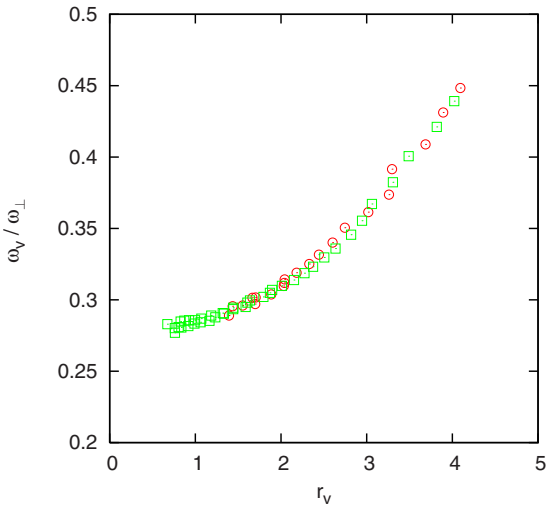

FIG. 5. (Color online) Precession angular frequency of the vortex, ω_v, in units of the radial trap frequency $\omega_\perp$, as a function of the radial position of the vortex, for $T/T_c=0.5$ and $N=10^4$. Results for two different initial vortex offset positions, $r_0=0.65a_\perp$ (squares) and $r_0=1.3a_\perp$ (circles), are illustrated. Note that near the center of the condensate ω_v changes little, but near the edge it changes rapidly.

Values of $\alpha=\gamma/\omega_v$ can therefore be estimated from γ in Fig. 4. The other necessary ingredient is ω_v, which can be calculated as a function of time using $\omega_v=x_v\dot{y}_v-y_v\dot{x}_v$, where the time derivatives are calculated numerically using central differences. Due to errors in locating the vortex position, there are large fluctuations in the calculated ω_v. To eliminate these fluctuations, we thus average results over two to three orbits of the vortex, corresponding to times $0<\omega_\perp t<50$. The resulting mean values are plotted in Fig. 6(a). These mean values are then used to calculate the values of α pre-

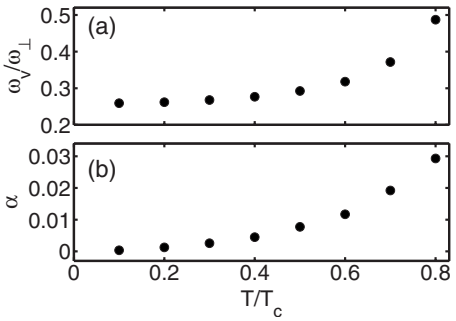

FIG. 6. (a) Precession angular frequency of the vortex, ω_v, in units of the radial trap frequency $\omega_\perp$ as a function of reduced temperature T/T_c. (b) Friction coefficient α as a function of T/T_c for a pancake trap geometry. The trap parameters are the same as in Fig. 2.

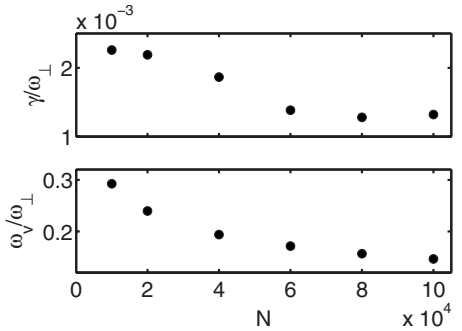

FIG. 7. (a) Decay rate γ and (b) precession frequency ω_v, as a function of total number of atoms N, for a temperature $T/T_c=0.5$ and a pancake trap geometry.

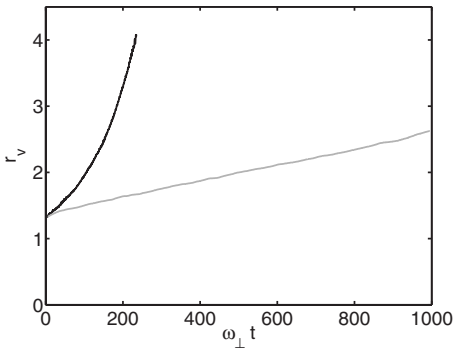

FIG. 8. Radial position of the vortex vs time for $T=0.6T_c$. The black line is the result with collisions, while the gray line is the result of a collisionless simulation as discussed in the text.

sented in Fig. 6(b). The observed increase in α with rising T is similar to the behavior observed in liquid ^{3}He [90] and ^{4}He [59,89].

Let us now investigate the role of the α' coefficient in Eq. (6). Experiments in liquid helium show a small effect, and there has been some controversy in the literature about this transverse component of the friction force [63–66]. This issue can be addressed within our simulations by comparing the "dynamic" thermal cloud frequency ω_v to a static value $\omega_{\rm st}$ found using a GP simulation in which the dynamics of the thermal cloud is ignored, that is, it retains its initial equilibrium form (in the absence of the vortex) for all times. In this *static thermal cloud approximation*, the thermal cloud exerts a time-independent mean-field potential on the condensate which modifies slightly the condensate density profile in the radial direction. This effect can be identified with the v_i/r_v term in Eq. (7), giving the simple relation $\alpha'=(1-\omega_v/\omega_{\rm st})$. We find that ω_v and $\omega_{\rm st}$ are equal to within 2–3 %, showing that the changes observed in ω_v in Fig. 6 are almost entirely due to the effects of the static thermal cloud potential on the condensate density profile and not to "real" dynamical effects associated with the time evolution of the thermal cloud density. The errors in measuring the vortex precession frequency are such that we cannot confidently extract a value for α' although our simulations indicate that $|\alpha'|<0.02$ throughout the measured temperature range $0<T/T_c<0.8$. This agrees with recent results of Berloff and Youd [97] obtained by means of classical field theory.

We also explore the dependence of these parameters on the total number of atoms, N. Figure 7 shows results for N between 10^4 and 10^5 and a fixed value of $T=0.5$ T_c. The decay rate γ, plotted in Fig. 7(a), decreases by about a factor of 2 over this range of N. The vortex precession frequency shown in Fig. 7(b) also has a decreasing trend, in agreement with what one would expect from GP solutions. These decreasing trends approximately cancel when calculating $\alpha=\gamma/\omega_v$, leading to values of α in the range of 0.8×10^{-2}–10^{-2} with no clear dependence on N.

C. Collisionless simulations

In general, damping in the ZNG formalism arises from the coupling of the condensate to the thermal cloud by means of mean-field interactions and C_{12} collisions. In order to explore the relative importance of these two contributions, we have performed simulations where collisions are not present, so $C_{12}=C_{22}=0$ in Eq. (2), and the only source of dissipation is mean-field coupling. Physically, this dissipation is a form of Landau damping whereby the motion of the vortex core through the thermal cloud generates thermal excitations [75]. In Fig. 8 the radial position for the collisionless simulation at $T=0.6T_c$ is shown as the gray line and compared to the collisional result in black. Without collisions one obtains a much slower decay, highlighting the crucial role of collisional damping in the simulations, a conclusion which has been numerically verified over a broad range of temperatures. The near linear variation in r_v with time seen in Fig. 8 indicates that an exponential function would be a poor fit to the data in this case.

D. Rotating thermal clouds

We also consider the case where, instead of being stationary initially, the thermal cloud undergoes solid-body rotation around the z axis with angular frequency $\Omega_{\rm th}$. The thermal cloud velocity at the vortex core is then $\mathbf{v}_n=\Omega_{\rm th}r_v\hat{\phi}$. Hence $\Omega_{\rm th}>0$ represents rotation in the same sense as the vortex precession, while $\Omega_{\rm th}<0$ corresponds to rotation in the opposite sense. Using Eq. (6) then yields

$$\omega_v=(1-\alpha')\frac{v_i}{r_v}+\alpha'\Omega_{\rm th} \tag{9}$$

and

$$r_v=r_0e^{\alpha(\omega_v-\Omega_{\rm th})t}. \tag{10}$$

For simulations involving a rotating thermal cloud, we start with the equilibrium condensate and thermal cloud distributions evaluated at $T=0.7T_c$ and $\Omega_{\rm th}=0$. A rigid-body rotation of the thermal cloud is then imposed by adding $\mathbf{v}_n=\Omega_{\rm th}r_v\hat{\phi}$ to each atom's velocity. It should be noted that the thermal cloud will now no longer be in "equilibrium" since there is a centrifugal effect which tends to expand the cloud. This initial outward expansion leads to an oscillation in the radial direction and, since angular momentum is conserved, a corresponding oscillation of the cloud's angular velocity.

The vortex decay curves are plotted in Fig. 9 for different $\Omega_{\rm th}$ and show that the decay rate increases for rotations op-

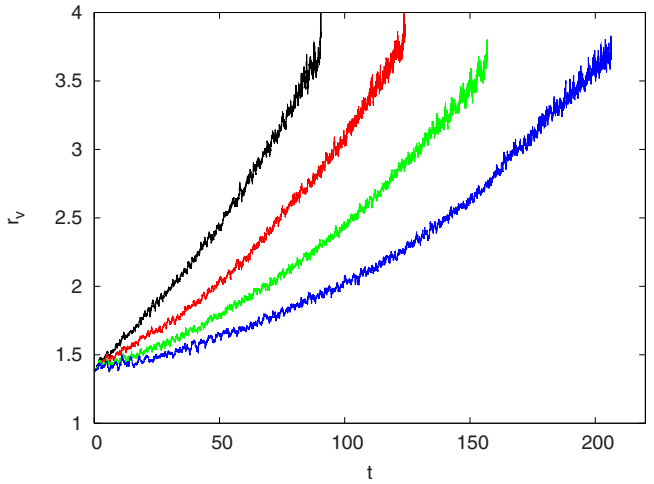

FIG. 9. (Color online) Time evolution of vortex radial position for $T=0.7T_c$ and a rotating thermal cloud. The different curves represent varying thermal cloud rotation rates, with $\Omega_{\rm th}=-0.2$ (black, top), $\Omega_{\rm th}=0$ (red), $\Omega_{\rm th}=0.2$ (green), and $\Omega_{\rm th}=0.37$ (blue, bottom).

posite to the vortex precession direction but decreases as the rotation rate is increased in the same direction. This is consistent with the expected behavior from Eq. (10). To study the problem more quantitatively, we again fit exponentials of the form ae^{bt} to the decay curves over $0\leq\omega_\perp t\leq 50$. The values of b for the different $\Omega_{\rm th}$ are plotted in Fig. 10. The straight line, $b=\alpha(\omega_v-\Omega_{\rm th})=\gamma(1-\Omega_{\rm th}/\omega_v)$, is the expected result from Eq. (10), where α and ω_v are taken from the results of the $\Omega_{\rm th}=0$ simulations found earlier. Our results are in quite good agreement with this behavior, although some small discrepancies are apparent. These could be due to the oscillations in $\Omega_{\rm th}$ noted earlier, whereas Eq. (10) assumes that $\Omega_{\rm th}$ is strictly time independent throughout the precessional motion of the vortex.

IV. CONCLUSIONS

In summary, we have studied the finite temperature dynamics of a single vortex in a partially condensed ultracold

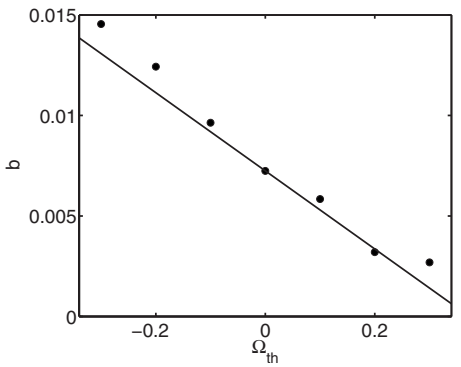

FIG. 10. Values of the decay rate b for different rotation rates of the thermal cloud, $\Omega_{\rm th}$. The solid line plots the function $b=\gamma(1-\Omega_{\rm th}/\omega_v)$ (where γ and ω_v are the decay rate and the precession angular velocity, respectively, for a nonrotating thermal cloud), which is the expected dependence from Eq. (10).

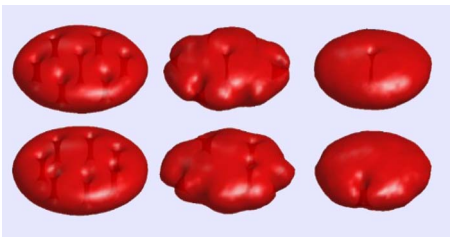

FIG. 11. (Color online). Vortex lattice decay at $T=0.7T_c$. The top row shows the time evolution (left to right) of a lattice with a vortex initially at the center; the bottom row shows the evolution of a lattice with the same number of vortices but having a ring configuration.

Bose gas. Our methodology and detailed simulations provide several advantages over previous studies. First, our simulations include the full effects of the trapping potential through the self-consistent determination of condensate and thermal cloud in the initial state. This results in a more realistic model as compared to those using the approximation of uniform densities [37,40,44]. The inclusion of nonuniform densities accounts more realistically for both the dynamics of the vortex and the positional dependence of the dissipation. Second, our model includes both mean-field [37] and collisional [44] dampings and allows us to compare the relative importance of the two mechanisms. Third, the thermal cloud is not assumed to be static as in earlier treatments [80] but is treated dynamically on the same footing as the condensate. In addition, our approach allows us to determine the effect on the damping rate of a thermal cloud moving relative to the condensate as, for example, when undergoing a rigid-body rotation.

A comparison of our results with those of other studies revealed some significant differences particularly with regard to the temperature dependence of the vortex relaxation rate. Furthermore, by analyzing the motion of the vortex near the trap center where the density is nearly constant, we were able to extract the mutual friction coefficients which appear in phenomenological vortex dynamics equations. Our simulations provide the *ab initio* determination of these coefficients in the context of a trapped Bose gas. In addition, the simulations provide some justification for the validity of the phenomenological equations themselves.

Our approach can also be extended to study the role of a dynamical thermal cloud on vortex lattice dynamics [98–100], thereby complementing and extending existing work [38–40,80,101–104]. To illustrate this possibility, we conclude by briefly reporting on some preliminary results for the decay of vortex lattices. We consider the evolution of two different vortex lattice configurations shown in Fig. 11. Both vortex arrays initially contain seven vortices (left images), however they differ in the way the vortices are arranged. The first array (top images) consists of one vortex at the center of the condensate and a ring of six vortices around it, whereas the second array (bottom) consists of a ring of seven vortices with no central vortex. These arrays rotate in the laboratory frame, and at finite temperatures, the effects of dissipation lead to the gradual one-by-one disappearance of the off-centered vortices. For simulations performed at $T=0.7T_c$, we

find that the array with all vortices arranged in a ring decays faster: after the first six vortices have decayed, the system is left with a single off-center vortex which moves relatively rapidly to the edge and disappears. This whole evolution occurs on a time scale $\omega_\perp t \simeq 150$. The decay rate in the simulations is in order-of-magnitude agreement with measurements performed on a bigger lattice [7] when the results for the latter are extrapolated to our value of T/T_c.

In contrast to this, the lattice with the central vortex reaches a point where a single metastable central vortex remains after the other six have been shed. This vortex also eventually decays, but our simulations suggest that the decay occurs on a much longer time scale. Some numerical experiments we have performed for configurations with no initial central vortex have exhibited a similar metastable behavior. If, during the initial part of the evolution (in which the vortices move irregularly), a vortex ends up sufficiently close to the center, it can become "stuck" near the center while the other vortices are shed. These observations are in agreement with reports [105] that the decay time of the last vortex is much longer than that of the initial vortex array.

We stress, however, that a more accurate treatment of the evolution of a metastable central vortex requires the explicit inclusion of stochastic noise to provide a kick, as discussed in [44,45]. Such a term was included in a recent discussion [104], however the thermal cloud was still treated as static. A combination of the stochastic Gross-Pitaevskii equation and the quantum Boltzmann equation may thus be needed to provide a more complete description of this particular situation. However, we expect that most other cases can be modeled extremely well by the Zaremba-Nikuni-Griffin approach. In particular, it would of interest to see if more detailed calculations of vortex lattice decay would be consistent with experimental observations [7]. Other applications might include the study of vortex lattice excitations (Tkachenko modes) [106] and the dynamics of bent vortices in elongated condensates [6].

ACKNOWLEDGMENTS

This work was funded by EPSRC under Grant No. EP/D040892/1 (B.J., N.P.P., and C.F.B.) and by NSERC (E.Z.).

[1] D. S. Jin, M. R. Matthews, J. R. Ensher, C. E. Wieman, and E. A. Cornell, Phys. Rev. Lett. **78**, 764 (1997).
[2] D. M. Stamper-Kurn, H.-J. Miesner, S. Inouye, M. R. Andrews, and W. Ketterle, Phys. Rev. Lett. **81**, 500 (1998).
[3] O. Maragò, G. Hechenblaikner, E. Hodby, and C. Foot, Phys. Rev. Lett. **86**, 3938 (2001).
[4] F. Chevy, V. Bretin, P. Rosenbusch, K. W. Madison, and J. Dalibard, Phys. Rev. Lett. **88**, 250402 (2002).
[5] S. Burger, K. Bongs, S. Dettmer, W. Ertmer, K. Sengstock, A. Sanpera, G. V. Shlyapnikov, and M. Lewenstein, Phys. Rev. Lett. **83**, 5198 (1999).
[6] P. Rosenbusch, V. Bretin, and J. Dalibard, Phys. Rev. Lett. **89**, 200403 (2002).
[7] J. R. Abo-Shaeer, C. Raman, and W. Ketterle, Phys. Rev. Lett. **88**, 070409 (2002).
[8] L. P. Pitaevskii, Zh. Eksp. Teor. Fiz. **35**, 408 (1958) [Sov. Phys. JETP **35**, 282 (1959)]; S. Choi, S. A. Morgan, and K. Burnett, Phys. Rev. A **57**, 4057 (1998).
[9] M. Tsubota, K. Kasamatsu, and M. Ueda, Phys. Rev. A **65**, 023603 (2002); E. J. M. Madarassy and C. F. Barenghi, J. Low Temp. Phys. **152**, 122 (2008).
[10] A. Griffin, Phys. Rev. B **53**, 9341 (1996).
[11] N. P. Proukakis and K. Burnett, J. Res. Natl. Inst. Stand. Technol. **101**, 457 (1996); N. P. Proukakis, K. Burnett, and H. T. C. Stoof, Phys. Rev. A **57**, 1230 (1998); N. P. Proukakis, J. Phys. B **34**, 4737 (2001).
[12] E. Zaremba, T. Nikuni, and A. Griffin, J. Low Temp. Phys. **116**, 277 (1999).
[13] R. Walser, J. Williams, J. Cooper, and M. Holland, Phys. Rev. A **59**, 3878 (1999); R. Walser, J. Cooper, and M. Holland, *ibid.* **63**, 013607 (2000).
[14] M. Imamovic-Tomasovic and A. Griffin, Phys. Rev. A **60**, 494 (1999).
[15] M. J. Bijlsma, E. Zaremba, and H. T. C. Stoof, Phys. Rev. A **62**, 063609 (2000).
[16] C. W. Gardiner, Phys. Rev. A **56**, 1414 (1997).
[17] Y. Castin and R. Dum, Phys. Rev. A **57**, 3008 (1998).
[18] S. A. Morgan, J. Phys. B **33**, 3847 (2000); S. A. Gardiner and S. A. Morgan, Phys. Rev. A **75**, 043621 (2007).
[19] B. V. Svistunov, J. Mosc. Phys. Soc. **1**, 373 (1991); Y. Kagan and B. V. Svistunov, Phys. Rev. Lett. **79**, 3331 (1997); Sov. Phys. JETP **75**, 387 (1992); N. G. Berloff and B. V. Svistunov, Phys. Rev. A **66**, 013603 (2002).
[20] M. J. Davis, S. A. Morgan, and K. Burnett, Phys. Rev. Lett. **87**, 160402 (2001); P. B. Blakie and M. J. Davis, Phys. Rev. A **72**, 063608 (2005).
[21] M. Brewczyk, M. Gajda, and K. Rzazewski, J. Phys. B **40**, R1 (2007).
[22] C. W. Gardiner and P. Zoller, Phys. Rev. A **58**, 536 (1998); **61**, 033601 (2000).
[23] H. T. C. Stoof, Phys. Rev. Lett. **78**, 768 (1997); J. Low Temp. Phys. **114**, 11 (1999); H. T. C. Stoof and M. J. Bijlsma, *ibid.* **124**, 431 (2001).
[24] C. W. Gardiner, J. R. Anglin, and T. I. A. Fudge, J. Phys. B **35**, 1555 (2002); C. W. Gardiner and M. J. Davis, *ibid.* **36**, 4731 (2003).
[25] N. P. Proukakis and B. Jackson, J. Phys. B **41**, 203002 (2008).
[26] P. B. Blakie, A. S. Bradley, M. J. Davis, R. J. Ballagh, and C. W. Gardiner, Adv. Phys. **57**, 363 (2008).
[27] B. Jackson and E. Zaremba, Phys. Rev. A **66**, 033606 (2002).
[28] B. Jackson and E. Zaremba, Phys. Rev. Lett. **87**, 100404 (2001).
[29] B. Jackson and E. Zaremba, Phys. Rev. Lett. **88**, 180402 (2002).
[30] B. Jackson and E. Zaremba, Phys. Rev. Lett. **89**, 150402 (2002).
[31] T. Nikuni and A. Griffin, Phys. Rev. A **63**, 033608 (2001).
[32] T. Nikuni and A. Griffin, Phys. Rev. A **69**, 023604 (2004).

[33] B. Jackson, N. P. Proukakis, and C. F. Barenghi, Phys. Rev. A **75**, 051601(R) (2007); B. Jackson, C. F. Barenghi, and N. P. Proukakis, J. Low Temp. Phys. **148**, 387 (2007).
[34] R. J. Dodd, K. Burnett, M. Edwards, and C. W. Clark, Phys. Rev. A **56**, 587 (1997).
[35] A. A. Svidzinsky and A. L. Fetter, Phys. Rev. Lett. **84**, 5919 (2000).
[36] E. Lundh and P. Ao, Phys. Rev. A **61**, 063612 (2000).
[37] P. O. Fedichev and G. V. Shlyapnikov, Phys. Rev. A **60**, R1779 (1999).
[38] O. N. Zhuravlev, A. E. Muryshev, and P. O. Fedichev, Phys. Rev. A **64**, 053601 (2001).
[39] P. O. Fedichev and A. E. Muryshev, Phys. Rev. A **65**, 061601(R) (2002).
[40] A. A. Penckwitt, R. J. Ballagh, and C. W. Gardiner, Phys. Rev. Lett. **89**, 260402 (2002).
[41] H. Schmidt, K. Góral, F. Floegel, M. Gajda, and K. Rzażewski, J. Opt. B: Quantum Semiclassical Opt. **5**, S96 (2003).
[42] Z. Hadzibabic, P. Krüger, M. Cheneau, B. Battelier, and J. Dalibard, Nature (London) **441**, 1118 (2006).
[43] T. P. Simula and P. B. Blakie, Phys. Rev. Lett. **96**, 020404 (2006); T. P. Simula, M. J. Davis, and P. B. Blakie, Phys. Rev. A **77**, 023618 (2008).
[44] R. A. Duine, B. W. A. Leurs, and H. T. C. Stoof, Phys. Rev. A **69**, 053623 (2004).
[45] R. Šášik, L. M. A. Bettencourt, and S. Habib, Phys. Rev. B **62**, 1238 (2000).
[46] *Quantized Vortex Dynamics and Superfluid Turbulence*, edited by C. F. Barenghi, R. J. Donnelly, and W. F. Vinen (Springer, Berlin, 2001).
[47] J. Maurer and P. Tabeling, Europhys. Lett. **43**, 29 (1998).
[48] W. F. Vinen and J. J. Niemela, J. Low Temp. Phys. **128**, 167 (2002).
[49] T. V. Chagovets, A. V. Gordeev, and L. Skrbek, Phys. Rev. E **76**, 027301 (2007).
[50] C. F. Barenghi, Physica D **237**, 2195 (2008).
[51] D. I. Bradley, D. O. Clubb, S. N. Fisher, A. M. Guenault, R. P. Haley, C. J. Matthews, G. R. Pickett, V. Tsepelin, and K. Zaki, Phys. Rev. Lett. **96**, 035301 (2006).
[52] M. Tsubota, T. Araki, and C. F. Barenghi, Phys. Rev. Lett. **90**, 205301 (2003).
[53] V. B. Eltsov, A. P. Finne, R. Hanninen, J. Kopu, M. Krusius, M. Tsubota, and E. V. Thuneberg, Phys. Rev. Lett. **96**, 215302 (2006).
[54] T. Lipniacki, Eur. J. Mech. B/Fluids **25**, 435 (2006).
[55] D. Kivotides, Phys. Rev. B **76**, 054503 (2007).
[56] D. C. Samuels and C. F. Barenghi, Phys. Rev. Lett. **81**, 4381 (1998).
[57] D. Kivotides, J. C. Vassilicos, D. C. Samuels, and C. F. Barenghi, Phys. Rev. Lett. **86**, 3080 (2001); W. F. Vinen, M. Tsubota, and A. Mitani, *ibid.* **91**, 135301 (2003); E. Kozik and B. Svistunov, *ibid.* **92**, 035301 (2004); S. Nazarenko, JETP Lett. **84**, 585 (2007).
[58] M. Leadbeater, T. Winiecki, D. C. Samuels, C. F. Barenghi, and C. S. Adams, Phys. Rev. Lett. **86**, 1410 (2001); C. F. Barenghi and D. C. Samuels, J. Low Temp. Phys. **136**, 281 (2004).
[59] C. F. Barenghi, R. J. Donnelly, and W. F. Vinen, J. Low Temp. Phys. **52**, 189 (1983).
[60] U. Frisch, *Turbulence* (Cambridge University Press, Cambridge, 1995).
[61] W. F. Vinen, Phys. Rev. B **71**, 024513 (2005).
[62] E. B. Sonin, Rev. Mod. Phys. **59**, 87 (1987).
[63] S. V. Iordanskii, Sov. Phys. JETP **22**, 160 (1966).
[64] E. B. Sonin, Sov. Phys. JETP **42**, 469 (1976).
[65] E. B. Sonin, Phys. Rev. B **55**, 485 (1997).
[66] P. Ao and D. J. Thouless, Phys. Rev. Lett. **70**, 2158 (1993).
[67] H. T. C. Stoof, M. Bijlsma, and M. Houbiers, J. Res. Natl. Inst. Stand. Technol. **101**, 443 (1996); M. Bijlsma and H. T. C. Stoof, Phys. Rev. A **55**, 498 (1997).
[68] N. P. Proukakis, S. A. Morgan, S. Choi, and K. Burnett, Phys. Rev. A **58**, 2435 (1998).
[69] H. Shi and A. Griffin, Phys. Rep. **304**, 1 (1998).
[70] D. A. W. Hutchinson, K. Burnett, R. J. Dodd, S. A. Morgan, M. Rusch, E. Zaremba, N. P. Proukakis, M. Edwards, and C. W. Clark, J. Phys. B **33**, 3825 (2000).
[71] F. Dalfovo, S. Giorgini, L. P. Pitaevskii, and S. Stringari, Rev. Mod. Phys. **71**, 463 (1999).
[72] L. P. Pitaevskii and S. Stringari, Phys. Lett. A **235**, 398 (1997).
[73] S. Giorgini, Phys. Rev. A **57**, 2949 (1998).
[74] M. Guilleumas and L. P. Pitaevskii, Phys. Rev. A **61**, 013602 (1999).
[75] B. Jackson and E. Zaremba, New J. Phys. **5**, 88 (2003).
[76] A. Minguzzi, S. Succi, F. Toschi, M. P. Tosi, and P. Vignolo, Phys. Rep. **395**, 223 (2004).
[77] B. Jackson, J. F. McCann, and C. S. Adams, Phys. Rev. A **61**, 013604 (1999).
[78] A. L. Fetter and J.-k. Kim, J. Low Temp. Phys. **125**, 239 (2001).
[79] N. G. Parker, N. P. Proukakis, C. F. Barenghi, and C. S. Adams, Phys. Rev. Lett. **92**, 160403 (2004).
[80] S. M. M. Virtanen and M. M. Salomaa, J. Phys. B **35**, 3967 (2002).
[81] T. Isoshima and K. Machida, Phys. Rev. A **59**, 2203 (1999).
[82] B. P. Anderson, P. C. Haljan, C. E. Wieman, and E. A. Cornell, Phys. Rev. Lett. **85**, 2857 (2000).
[83] H. T. C. Stoof (private communication).
[84] R. A. Duine and H. T. C. Stoof, Phys. Rev. A **65**, 013603 (2001).
[85] R. A. Duine (private communication).
[86] R. J. Donnelly, *Quantized Vortices in Helium II* (Cambridge University Press, Cambridge, 1991).
[87] H. E. Hall and W. F. Vinen, Proc. R. Soc. London, Ser. A **238**, 215 (1956).
[88] K. W. Schwarz, Phys. Rev. B **38**, 2398 (1988).
[89] R. J. Donnelly and C. F. Barenghi, J. Phys. Chem. Ref. Data **27**, 1217 (1998).
[90] T. D. S. Bevan, A. J. Manninen, J. B. Cook, H. Alles, J. R. Hook, and H. E. Hall, J. Low Temp. Phys. **109**, 423 (1997).
[91] C. F. Barenghi, S. Hulton, and D. C. Samuels, Phys. Rev. Lett. **89**, 275301 (2002).
[92] C. F. Barenghi, R. J. Donnelly, and W. F. Vinen, Phys. Fluids **28**, 498 (1985).
[93] C. F. Barenghi, A. V. Gordeev, and L. Skrbek, Phys. Rev. E **74**, 026309 (2006).
[94] P. Lucas, J. Phys. C **3**, 1180 (1970).
[95] A. P. Finne, T. Araki, R. Blaauwgeers, V. B. Eltsov, N. B. Kopnin, M. Krusius, L. Skrbek, M. Tsubota, and G. E. Volovik, Nature (London) **424**, 1022 (2003).
[96] A. P. Finne, S. Boldarev, V. B. Eltsov, and M. Krusius, J. Low

Temp. Phys. **138**, 567 (2005).
[97] N. G. Berloff and A. J. Youd, Phys. Rev. Lett. **99**, 145301 (2007).
[98] K. W. Madison, F. Chevy, W. Wohlleben, and J. Dalibard, Phys. Rev. Lett. **84**, 806 (2000).
[99] J. R. Abo-Shaeer, C. Raman, J. M. Vogels, and W. Ketterle, Science **292**, 476 (2001).
[100] E. Hodby, G. Hechenblaikner, S. A. Hopkins, O. M. Marago, and C. J. Foot, Phys. Rev. Lett. **88**, 010405 (2001).
[101] C. Lobo, A. Sinatra, and Y. Castin, Phys. Rev. Lett. **92**, 020403 (2004).
[102] M. Tsubota, K. Kasamatsu, and M. Ueda, Phys. Rev. A **65**, 023603 (2002); K. Kasamatsu, M. Machida, N. Sasa, and M. Tsubota, *ibid.* **71**, 063616 (2005).
[103] S. M. M. Virtanen, T. P. Simula, and M. M. Salomaa, Phys. Rev. Lett. **86**, 2704 (2001).
[104] A. S. Bradley, C. W. Gardiner, and M. J. Davis, Phys. Rev. A **77**, 033616 (2008).
[105] V. Bretin, P. Rosenbusch, F. Chevy, G. V. Shlyapnikov, and J. Dalibard, Phys. Rev. Lett. **90**, 100403 (2003).
[106] I. Coddington, P. Engels, V. Schweikhard, and E. A. Cornell, Phys. Rev. Lett. **91**, 100402 (2003).